

# Critical Behavior of the Three-Dimensional Random Anisotropy Heisenberg Model

J.J. Ruiz-Lorenzo,<sup>1,2</sup> M. Dudka,<sup>3,4</sup> and Yu. Holovatch<sup>3,4,5</sup>

<sup>1</sup> *Departamento de Física and Instituto de Computación Científica Avanzada (ICCAEx),  
Universidad de Extremadura, 06071 Badajoz, Spain.*

<sup>2</sup> *Instituto de Biocomputación y Física de Sistemas Complejos (BIFI), 50018 Zaragoza, Spain.*

<sup>3</sup> *Institute for Condensed Matter Physics, National Acad. Sci. of Ukraine, UA-79011 Lviv, Ukraine*

<sup>4</sup><sup>L</sup> *Collaboration & Doctoral College for the Statistical Physics of Complex Systems, Leipzig-Lorraine-Lviv-Coventry, Europe*

<sup>5</sup> *Centre for Fluid and Complex Systems, Coventry University, Coventry, CV1 5FB, United Kingdom*

(Dated: December 28, 2021)

We have studied the critical properties of the three-dimensional random anisotropy Heisenberg model by means of numerical simulations using the Parallel Tempering method. We have simulated the model with two different disorder distributions, cubic and isotropic ones, with two different anisotropy strengths for each disorder class. We have obtained clear signatures of a second order phase transition (paramagnetic-ferromagnetic) for the cubic and the isotropic disorder distributions and we have characterized the critical exponents and cumulants. In the case of isotropic disorder distribution we have found a strong dependence of the thermal exponent on the disorder strength. Finally, we have found evidences of universality for the case of the anisotropic disorder distribution by finding critical exponents and universal dimensionless ratios independent of the strength of the disorder.

## I. INTRODUCTION

Structurally disordered systems apart from fundamental interests are also important for modern technology. For instance recently developed rare-earth based magnetic glasses with magnetocaloric effects were considered as good candidates for magnetic refrigerants [1]. These rare-earth based systems belong to a wide class of disordered materials [2, 3] known as random-anisotropy magnets.

Magnetic properties of these systems are described by random anisotropy model (RAM), in which each spin is subjected to a local anisotropy of random orientation with the Hamiltonian [4]:

$$\mathcal{H} = -J \sum_{\langle \mathbf{r}, \mathbf{r}' \rangle} \mathbf{S}_{\mathbf{r}} \cdot \mathbf{S}_{\mathbf{r}'} - D \sum_{\mathbf{r}} (\hat{\mathbf{x}}_{\mathbf{r}} \cdot \mathbf{S}_{\mathbf{r}})^2. \quad (1)$$

Here,  $\mathbf{S}_{\mathbf{r}}$  is a classical  $m$ -component unit vector on the site  $\mathbf{r}$  of a  $d$ -dimensional (hyper)cubic lattice,  $D > 0$  is the strength of the anisotropy,  $\hat{\mathbf{x}}_{\mathbf{r}}$  is a (quenched) random unit vector pointing in the direction of the local anisotropy axis. The interaction  $J > 0$  is assumed to be ferromagnetic. We consider the case of short-range interactions, with  $\langle \cdot, \cdot \rangle$  meaning summation over pairs of nearest neighbors. The strength of the disorder is controlled by the ratio  $D/J$ . Obviously, the random orientations are present in the model (see Eq. (1)) only for  $m > 1$ . In the case  $m = 1$  the random anisotropy term becomes constant and leads only to a shift of the Ising system free energy.

Experimental data from random anisotropy systems are accessible from reviews, see for instance Refs. [5, 6]. The RAM was also an object of extensive theoretical and numerical studies reviewed in Refs. [7, 8]. Despite the efforts made so far, the problem of the nature of a low-temperature phase in random anisotropy magnets remains a most controversial issue. In particular, the

question of whether the low-temperature phase is long-range ferromagnetically ordered or is it a spin-glass. Local anisotropy prevents fully ferromagnetic state, where all spins align in the same direction. Therefore the term ‘asperomagnetic’ was proposed for magnetically ordered low-temperature state with non-zero magnetisation, while the term ‘speromagnetic’ was coined for the spin-glass like state with zero magnetisation [9]. Within phenomenological theory the last state is also called ‘correlated spin-glass’ [10]. Another possible candidate for the low-temperature phase in RAM is a quasi long-range order (QLRO), i.e. the low temperature ordering typical for the Berezinskii-Kosterlitz-Thouless transition [11, 12], where the pair correlation function is characterized by a power-law decay with distance while the magnetization is zero.

Influence of the local anisotropy axis distributions on the critical behavior of RAM is of particular interest. The studies performed so far agree on the fact that the form of the distribution is crucial for the critical behavior of RAM. In the next section we will review results of previous studies. We will concentrate mainly on the two mentioned issues: origin of the low-temperature phase and the role of the local anisotropy axis distribution. We will leave out of scope several other challenging topics, as dynamical aspects of phase transitions in RAM [13], effects of long-range correlations of local anisotropy axes [14] or the presence of a surface [15].

We will do this with a purpose to emphasize the main goal of our paper: In the current situation it is of primary importance to apply the state-of-the-art numerical techniques to get a high accuracy quantitative description of the critical behavior of three-dimensional Heisenberg model with moderate quenched random anisotropy in order to confront predictions of the most recent analytic calculations based on perturbative renormalization group (RG).

To this end, we will use the Parallel Tempering (PT) method and carefully study low-temperature behavior of three-dimensional RAM at  $m = 3$  for two different local anisotropy axis distributions, the discrete and the continuous one, taking different values of the anisotropy strength for each distribution.

The outline of the rest of the paper is as follows. We review theoretical and numerical studies of RAM focusing mainly on results for the three-dimensional case in Section II. Next, we will describe our numerical simulations (simulating two different distributions of anisotropy axis) in Section III. Our results are displayed in Section IV and finally we will discuss them and state the conclusions in the last Section V. Technical details of numerical simulations, the description of the analysis methods and the numerical study of the three-dimensional  $O(3)$  model and the two-dimensional  $O(2)$  model (as a proxy of a model with QLRO) are described in four Appendices.

## II. REVIEW

### A. Theoretical results

First, we will describe the theoretical results regarding the isotropic disorder distribution.

The earliest theoretical investigations of the RAM were performed within the mean field framework. Ferromagnetism was predicted [4, 16] but the possibility of a spin-glass phase [17] was not excluded. Exact solution of the infinite-range interaction limit of the RAM within the mean-field approach indicates a second-order phase transition to ferromagnetic phase [18]. Such transition was also corroborated by  $1/d$ -expansions [19], as well as within mean-field and RG for  $m = 2$  case [20]. However local mean field theory [21] predicts the breakdown of long range ferromagnetic order.

Following the arguments of Imry and Ma [22] formulated for the random-field model it was shown that the  $d = 3$  random anisotropy magnet should break into magnetic domains of size  $L \sim (J/D)^2$  [23] for weak anisotropy and thus no ferromagnetism was expected. We will discuss this point in more details in Section II C.

Account of fluctuations within the field theoretical RG approach [24] leads to an absence of phase transition. In the pioneer RG calculations performed for RAM with *isotropic distribution* of  $\hat{\mathbf{x}}_r$  [25] no stable accessible fixed point of the RG transformation was found in the first order of the  $\varepsilon = 4 - d$ -expansion. Moreover, the effective Hamiltonian for such distribution at large  $D$  was shown to reduce to one that is similar to the effective Hamiltonian of the random-bond Ising spin glass [26], demonstrating a possibility of a spin glass phase in this case.

Several arguments were used in order to demonstrate an absence of the ferromagnetic order for space dimensions  $d < 4$  in RAM [27]. Although among these arguments the one for the limit  $m \rightarrow \infty$  [27] appeared

to be erroneous [28], the lack of ferromagnetism for the RAM with *isotropic distribution* of anisotropy axes for  $d < 4$  was further supported by a Mermin-Wagner type proof [29] using the replica trick [30] for  $m = 2$  case. The perturbative Migdal-Kadanoff RG studies [27, 28] also suggested dimensional reduction for RAM: critical behavior of this random system at  $d > 4$  is the same as for the corresponding pure system with dimension  $d - 2$ .

The one-loop result [25] about absence of the second order phase transition into ferromagnetic state was corroborated by two- [3, 8, 31, 32] and five-loop [33] calculations within the field-theoretical RG refined by resummation techniques.

The infinitely strong anisotropy limit of the RAM (which makes spins to be frozen in directions of local anisotropy axes and the Hamiltonian to be similar to that of the Ising random-bond spin glass model) was investigated with the help of high-temperature expansions. Results of a Padé-analysis [34] indicated typical spin glass behavior for space dimension  $d = 3$ , while in Ref. [35] after obtaining non power-law divergence of susceptibility of three-dimensional RAM for  $m = 2$  and no divergence in the case  $m = 3$  it was concluded that the lower critical dimension for the RAM with  $m = 2$  is  $d_L = 3$ .

The series analysis of Ref. [36] of the RAM in the infinitely strong anisotropy limit on Cayley-trees predicted ferromagnetic order, occurring for the number of nearest neighbors  $\tilde{z} > m$  and a spin glass order for  $\tilde{z} < m$ . Results obtained in the same study [36] by Migdal-Kadanoff position space RG corroborate this outcome:  $d = 3$  ferromagnetic order for small  $m$ , while for large  $m$  spin-glass phase is obtained in the same universality class as that of the Ising spin glass with randomly distributed couplings.

Investigations of the RAM in the spherical model limit  $m \rightarrow \infty$  were concentrated on the question about the possibility of a spin glass phase. This limit was studied by  $1/m$ -expansions [37–40] first. Within the replica method, a spin glass phase was found below  $d = 4$  for arbitrary  $D$  [37, 41]. Later, the spin glass solution was shown to be unstable [38]. A stable non-replica-symmetric solution was obtained for spin glass phase for  $d < 4$  [39]. However, the study of dynamics of spin glass order parameter avoiding replica method for the RAM shows an instability of the spin glass phase [40]. These results found their confirmation in the mean field treatment of the  $m \rightarrow \infty$  limit [42], where the spin glass phase appeared only as a feature of this limit and no spin glass phase was obtained for finite  $m$ . In the spherical limit a ferromagnetic order was obtained for  $d > 2$  and for  $D$  less than some critical value  $D_c$ , while for  $D$  larger  $D_c$  a spin glass phase was obtained for arbitrary  $d$  ( $D_c = 0$  for  $d \leq 2$ ) [43].

An equation of state of the RAM showing a zero magnetization and an infinite magnetic susceptibility in the low-temperature phase for any  $m$  was obtained perturbatively [44]. Two-spin correlations in this phase possess a power law decay. As mentioned above, such phase appears to be QLRO. The estimate of the susceptibility of the low-temperature phase was corrected using scaling

arguments [45] and it was found to be  $\chi \sim (D/J)^{-4}$  at  $d = 3$ . A similar dependence of the susceptibility was obtained by other approaches [10, 37]. The power law decay of spin correlations in the low-temperature phase was obtained in particular for harmonic system with random fields [46], which is an approximation of model with  $m = 2$  if vortices are neglected. But the last result is in disagreement with calculations [47] for model with random  $p$ -fold fields (for two-component fields and  $p = 2$  it corresponds to the RAM with the two-component order parameter) where spin-glass phase was obtained.

The QLRO [48] was found for the RAM with  $m = 3$  by the functional RG approach in the first order of  $\varepsilon = 4 - d$  expansion. The functional RG study of higher rank anisotropies argued that dimensional reduction breaks down [49]. It was corroborated within two-loop functional RG [50, 51]. These studies also showed that QLRO exists for RAM at  $d_{LC}^* < d < 4$  and  $m < 9,4412$ . Estimates based on expansions in  $\varepsilon$  and  $m - m^*$  predict  $d_{LC}^* > 3$ , however results obtained for small  $\varepsilon$  and  $m - m^*$  should be extrapolated for large deviations with caution, as pointed in Ref. [51]. Conditions for holding dimensional reduction were studied by  $1/m$ -expansions within the functional RG [52]. In Ref. [53] it was stated that all previous studies using  $1/m$ -expansions are not completely correct, since they do not take the large  $m$ -limit of the easy axes into account. However only the case of  $D < 0$  was of main interest in that study. Recent research of the large- $m$  limit reported glassy character of zero-temperature state [54].

The phenomenological theory [10] based on the continuous-field version of the Hamiltonian (Eq. (1)) and assuming correlations between randomly oriented anisotropy axes turned out to be a more appropriate approach for the interpretation of the field dependence of the experimentally observed magnetization in the ordered phase. In this approach the spin correlation function in different regimes of applied fields were analyzed [10]. In particular, the correlation length for small and zero fields was found to have the form  $\xi \sim R_a (\frac{J}{R_a D})^2$ , where  $R_a$  is the correlation range for random axes. Such a phase was called a correlated spin-glass phase.

Once we have discussed the isotropic disorder distribution, we will discuss the *anisotropic* case.

It was firstly investigated in a RG study [25] with a distribution of anisotropic axes, restricting directions of the axes along the hypercube edges (*cubic distribution*). No accessible stable fixed point corresponding to a second order phase transition point was found. Despite this, the possibility of a second order phase transition into a ferromagnetic phase with critical exponents of the diluted quenched Ising model for the RAM with a cubic distribution was pointed out in Ref. [56], where a more general case was considered. Such peculiarities were observed for a more general model [57] including the RAM with *cubic distribution* of random axes as a particular case. Subsequently, this result was corroborated within a two-loop RG calculations with resummation [3, 8, 32, 55] done di-

rectly for the RAM with *cubic distribution* showing that the critical behavior belongs to the universality class of the site-diluted Ising model. This result was further confirmed on the basis of a five-loop massive RG calculations [33]. While study of RAM with generic distribution [56, 57], including *isotropic* and *cubic* distributions as particular cases, within the RG approach followed by resummation has predicted continuous phase transition of new universality class [58], later it was demonstrated that this conclusion was based on the erroneous calculations [59].

The RAM in the infinite anisotropy limit with mixed isotropic and cubic distributions was also investigated by mean-field theories [60–62]. It was found that the presence of a random cubic anisotropy stabilizes the ferromagnetic phase [60]. Study in the limit  $m \rightarrow \infty$  with finite  $\alpha \equiv m/N$ , where  $N$  is number of spins (so called  $\alpha$ -limit) [62] gives phase diagrams with ferromagnetic, spin-glass phases as well as with mixed phase where both ferromagnetic and spin-glass order parameters are non-zero.

Summing up, from the analysis of theoretical results one may conclude that while for isotropic distribution absence of ferromagnetic ordering is expected, such ordering is possible for anisotropic distribution of the local anisotropy axis.

## B. Numerical results

Most of the performed numerical simulations of the  $d = 3$  RAM study the cases  $D/J > 1$  or more often the infinitely strong anisotropy ( $D/J \rightarrow \infty$ ) limit.

Earliest investigations report inconclusive results: both stability [63, 64] as well as instability [65, 66] of the ferromagnetic order with respect to the spin-glass phase has been reported. However, data of later investigations indicated the absence of ferromagnetism.

The restriction to the infinitely strong anisotropy limit led to a lack of long-range order in the ground state for  $m = 3$  [67]. In this case, the critical exponents at the transition to a low-temperature phase were reported to be similar to those of the three-dimensional short-range Ising spin glass [68]. Results of Monte Carlo simulations [69] confirmed an absence of long-range order. Finally most recent study of the infinitely strong anisotropy limit of RAM with  $m = 3$  convincingly shows that the model in this case belongs to the class of short-range Ising spin-glass with bond disorder [70].

On the other hand, results of Monte Carlo study of the infinitely strong anisotropy limit of RAM with  $m = 2$  show a low-temperature phase with extremely large susceptibility, power law decay of the correlations and vanishing magnetization [69], that is consistent with the theoretically predicted QLRO for arbitrary  $m$  and weak anisotropy [44]. That is confirmed by result of Ref. [71], where a sharp phase transition into a low-temperature phase with power-law decay of the correlation function

and no true magnetization were found. This case was also studied in the infinite anisotropy limit [72] of model with random 2-fold fields, where weak ferromagnetic order was found with power-law correlations.

Numerical simulations of RAM with finite ratio of  $D/J$  reported the phase transition into spin-glass phase for the model with random 2-fold fields at  $J = D$  [73]. Another Monte Carlo study of the RAM (1) with  $m = 2$  and  $J = D$  resulted in critical exponents with values similar to the XY-ferromagnetic transition, except that the heat capacity critical exponent was found to be positive [74].

Performing Monte Carlo calculations for the RAM Hamiltonian (1) with  $m = 3$  and several values of  $D/J$  as well as at  $D/J \rightarrow \infty$  the phase diagram in the plane  $(D/J, T/J)$  was found [75]. There, the regions of existence of magnetic and spin-glass orders were indicated, with general conclusion that random anisotropy Heisenberg model for small  $D/J$  has QLRO low-temperature phase characterized by frozen power law spin correlations.

Results of study of the model with random 2-fold fields at several values of  $D/J$  suggest that system is ferromagnetic in low temperature phase at finite values of  $D/J$  [76].

Results reviewed above concern cases of continuous symmetry of the order parameter. Below we consider cases where orientations of spins as well as of the local anisotropy axes are limited only to several directions in  $m$ -dimensional space. In particular, studying RAM with  $m = 2$ , where the spins and anisotropic axes are oriented along the edges of a cube, the conventional XY second order phase transition to the ferromagnetic phase was found for weak random anisotropy [77], whereas a first-order transition to a domain type ferromagnetic phase was found for strong random anisotropy. For  $m = 3$  both transitions were found to be of the first order [77].

The possibility of the existence of a QLRO phase was also obtained for  $m = 3$  in the case of weak anisotropy but assuming  $D/J = \infty$  for a part  $q$  of sites and  $D/J = 0$  for the rest of  $1 - q$  sites [78]. There, the spins and anisotropic axes were chosen from the 12 directions. Results indicate, that in addition to paramagnetic and the ferromagnetic ordering a QLRO phase appears as an intermediate phase for some values of  $q$ .

The RAM with two-component spins is adopted to describe six-state clock model, where direction of spins belongs to  $Z_6$  group, while local anisotropy orientation are taken from  $Z_3$  group. The obtained low-temperature phase in this model has two-spin correlations decaying according to a power law, but no long-range magnetic order [79].

To summarize, the reviewed numerical studies agree, in general, with the theoretical predictions about the absence of long-range order for the  $d = 3$  RAM with isotropic random axes distribution. However, they show the possibility of a ferromagnetic order for the cases where orientations of local anisotropy axes are limited only to several directions.

An exception is given by the study of RAM with Heisenberg spins ( $m = 3$ ) [80]. Studying the case  $D/J=4$  for *isotropic* distribution and *cubic* distributions surprisingly second-order phase transition to ferromagnetically ordered state (mistakenly identified as QLRO) was found with the same correlation length critical exponent. To check this outcome we perform similar computations for larger lattices and for two values of  $D/J$ . But before describing our model let us go back to the cornerstone of argumentation of an absence of long-range order for  $d = 3$  RAM, the Imry-Ma arguments.

### C. Imry-Ma arguments

Imry and Ma introduced domain arguments in order to understand the low temperature phase of random field magnets [22]. Later, similar arguments were directly applied to the random anisotropy case [6, 23, 48].

Existence of random directions in the RAM system can lead it to splitting into domains inside which spins are directed almost along one direction. If the typical size of the domains is  $L$ , than energy gain for system is  $\sim DL^{d/2}$ . Whereas the loss of the surface energy per domain for the continuous symmetry order parameter can be estimated as  $\sim JL^{d-2}$ . Minimizing total energy from these two contributions with respect to  $L$  one gets  $L \sim (J/D)^{2/4-d}$ . That means that even for very small anisotropy strength RAM always should split into domain for  $d < 4$ . Earlier similar result was obtained by Larkin [81] in the context of vortex lattice in a superconductor. Therefore one can find different names of typical size of domains: Larkin length, Imry-Ma length or Imry-Ma-Larkin length.

Validity of these arguments were questioned. Berzin, Morosov and Sigov [82] pointed that random-field arguments can not be directly applied to the random-anisotropy case since the orientations of  $\hat{x}_r$  in some direction of the order parameter space and opposite to it are equivalent in RAM. Moreover considering continuous field variant of the RAM they have shown that the long-range order is possible when the distribution of  $\hat{x}_r$  deviates from the isotropic one as well as the local anisotropy axis is present only on the part of sites [83].

Fisch [76] pointed that with presence of random vectors  $\hat{x}_r$  the random anisotropy system is not longer translationally invariant. Therefore the consideration that the twist energy at the boundary scales in the same way as in non-random magnets, i.e.  $\sim L^{d-2}$ , is not correct.

## III. THE MODEL AND SIMULATIONS

We have studied the Hamiltonian given by Eq. (1) with  $m = 3$  on a three-dimensional lattice of linear size  $L$  and volume  $V = L^3$  with periodic boundary conditions.

### A. Random axis distributions

Two kinds of disorder have been simulated. In the first case, called hereafter ‘isotropic disorder’, the random anisotropy vectors  $\hat{\mathbf{x}}_{\mathbf{r}}$  have a uniform probability distribution on the sphere of unit radius

$$p(\hat{\mathbf{x}}) = \frac{1}{4\pi}. \quad (2)$$

The results obtained for such disorder will be marked in the figures and tables as IRAM.

In the second case, called cubic or ‘anisotropic disorder’ and marked hereafter with ARAM, the vectors  $\hat{\mathbf{x}}_{\mathbf{r}}$  point along the six semi-axes of the cubic lattice with the same probability 1/6:

$$p(\hat{\mathbf{x}}) = \frac{1}{6} \sum_{i=1}^3 \left( \delta^{(3)}(\hat{\mathbf{x}} - \hat{\mathbf{k}}_i) + \delta^{(3)}(\hat{\mathbf{x}} + \hat{\mathbf{k}}_i) \right), \quad (3)$$

where the  $\hat{\mathbf{k}}_i$  ( $i = 1, 2, 3$ ) are the three unit vectors pointing to the three principal directions of a cubic lattice and  $\delta^{(3)}(\hat{\mathbf{x}})$  are Kronecker deltas. In our numerical calculations we fix  $J = 1$ , therefore anisotropy strength determines the ratio  $D/J$ . We measure temperature  $T$  in units of Boltzmann constant  $k_B$  and work mainly with the inverse temperature  $\beta = 1/T$ .

We have run Monte Carlo numerical simulations using the Metropolis (with 10 hits) and parallel tempering algorithms, see Refs. [84, 85]. We have simulated  $L = 6, 8, 12, 16, 24, 32$  and 48 cubic lattice sizes. See appendix A for more details on the parameters used in our runs and on the thermalization tests.

### B. Observables

We have simulated in this work only the vector channel (vector magnetization) of the model. The magnetization is computed as

$$M = \left\langle \sqrt{\mathcal{M}^2} \right\rangle, \quad (4)$$

with

$$\mathcal{M} = \frac{1}{V} \sum_{\mathbf{r}} \mathbf{S}_{\mathbf{r}}, \quad (5)$$

where, as usual,  $\langle \langle \dots \rangle \rangle$  is the thermal average and  $\overline{(\dots)}$  denotes the average over the disorder.

Calculating powers of  $\mathcal{M}$  we can get the associated susceptibility

$$\chi = V \overline{\langle \mathcal{M}^2 \rangle}, \quad (6)$$

and the Binder cumulant

$$U_4 = 1 - \frac{1}{3} \frac{\overline{\langle (\mathcal{M}^2)^2 \rangle}}{\overline{\langle \mathcal{M}^2 \rangle}^2}. \quad (7)$$

A definition of the correlation length on a finite lattice is [86]:

$$\xi = \left( \frac{\chi/F - 1}{4 \sin^2(\pi/L)} \right)^{\frac{1}{2}}, \quad (8)$$

where  $F$  is defined as the Fourier transform of the magnetization via

$$\mathcal{F}(\mathbf{k}) = \frac{1}{V} \sum_{\mathbf{r}} e^{i\mathbf{k} \cdot \mathbf{r}} \mathbf{S}_{\mathbf{r}} \quad (9)$$

with

$$F = \frac{V}{3} \overline{\langle |\mathcal{F}(2\pi/L, 0, 0)|^2 + \text{two permutations} \rangle}. \quad (10)$$

For a finite system of size  $L$ , the Binder cumulant obeys:

$$U_4(\beta, L) = f((\beta - \beta_c)L^{1/\nu}) + O(L^{-\omega}), \quad (11)$$

where  $\nu$  is the correlation length critical exponent,  $\omega$  is the leading correction to scaling and  $f(\cdot)$  is a scaling function. Neglecting scaling corrections, the curves of the Binder cumulant as a function of the temperature for two different lattice sizes intersect in one point, indicating the approximate location of critical temperature  $\beta_c$ . The same behavior is expected for the dimensionless cumulant defined as a ratio of the correlation length to system size,  $R_\xi = \xi/L$ .

We have also computed the derivatives of the Binder cumulant ( $\partial_\beta U_4$ ) and the correlation length ( $\partial_\beta \xi$ ) by computing connected average values of different moments of the magnetization (and  $\mathcal{F}$  in the case of  $\xi$ ). The derivative for quantity  $\mathcal{O}$  is calculated with the help of the total energy  $\mathcal{E}$  defined by Eq.(1):

$$\partial_\beta \overline{\langle \mathcal{O} \rangle} = \overline{\partial_\beta \langle \mathcal{O} \rangle} = \overline{\langle \mathcal{O} \mathcal{E} - \langle \mathcal{O} \rangle \langle \mathcal{E} \rangle}. \quad (12)$$

We have also corrected the bias of having a relatively small number of measures per sample: to do that we have applied a third order extrapolation as described in Ref. [87].

Finally, we have computed the  $g_2$  cumulant, which measures the lack of self-averaging of the system, defined as

$$g_2 = \frac{\overline{\langle \mathcal{M}^2 \rangle^2} - \overline{\langle \mathcal{M}^2 \rangle}^2}{\overline{\langle \mathcal{M}^2 \rangle}^2}. \quad (13)$$

If  $g_2$  goes to zero when system size  $L$  increases then susceptibility is a self averaging quantity. Otherwise the susceptibility does not self average (for details, see e.g., Ref. [88]).

## IV. RESULTS AND ANALYSIS

In Figs. 1 and 2 we show the behavior of  $R_\xi$  as a function of the inverse temperature  $\beta$  for the four simulated

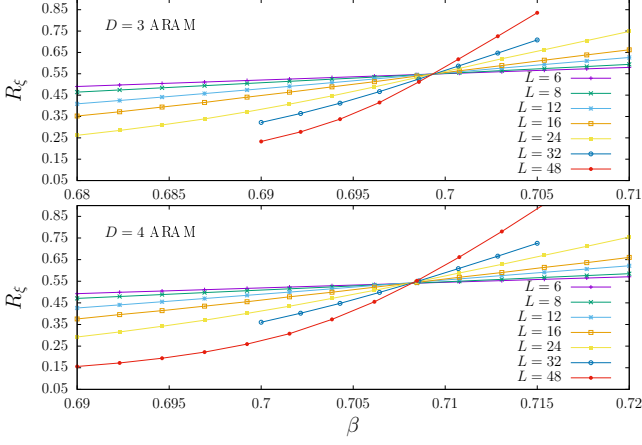


FIG. 1: (color online)  $R_\xi$  cumulant versus inverse temperature,  $\beta$ , for the cubic disorder for several lattice sizes.

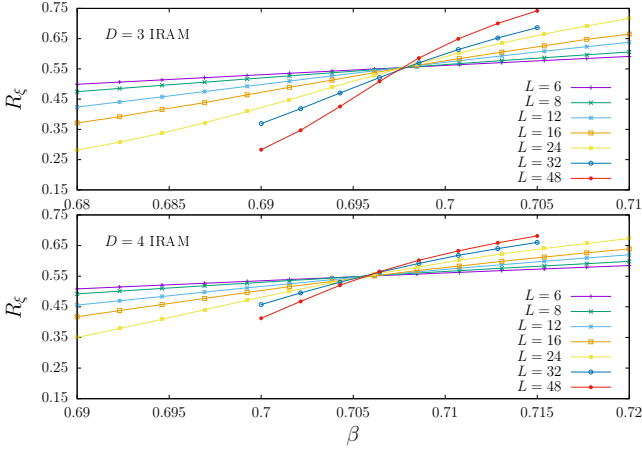


FIG. 2: (color online)  $R_\xi$  cumulant as a function of the inverse temperature for the isotropic disorder for several lattice sizes.

models (ARAM/IRAM and  $D = 3$  and  $4$ ). We also show the behavior of the Binder cumulant in Figs 3 and 4: the signature of a phase transition is really strong in all four models for both observables, Binder cumulant and correlation length. This is manifested by the crossing of the curves for different lattice sizes near the critical point.

In addition, we have also plotted in Figs. 5 and 6, the  $g_2$  cumulant. This cumulant shows clear crossing points (but much noisier than  $R_\xi$  and  $U_4$ ), which do not extrapolate to zero (see below). This is a strong signature that these four models do not belong to the same universality class of a pure or non-disordered model ( $g_2 = 0$ ).

Once we have found the phase transitions in the four models, we have analyzed quantitatively the behavior of the different observables using the quotient and the fixed coupling methods (see the Appendix B for a description of these methods).

We have computed the crossing points of the  $R_\xi(\beta, L)$  or Binder curves of  $L$  and  $2L$  lattices:  $R_\xi(\beta_{\text{cross}}(L, 2L), L) = R_\xi(\beta_{\text{cross}}(L, 2L), 2L)$  or

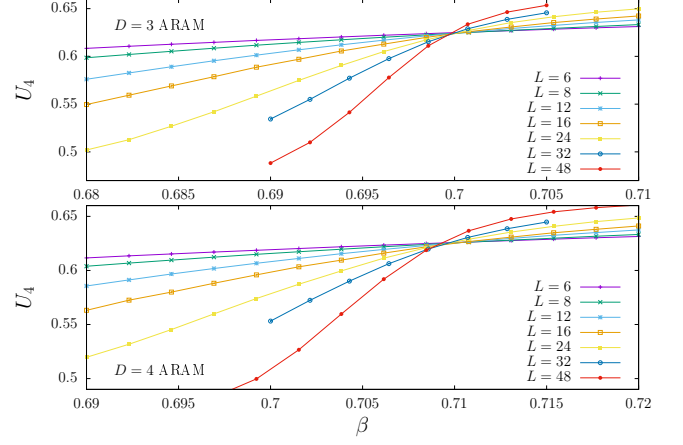


FIG. 3: (color online) Binder cumulant versus inverse temperature for the cubic disorder for several lattice sizes.

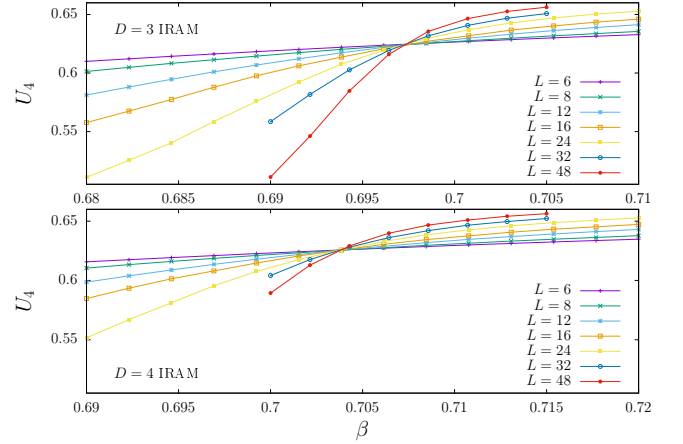


FIG. 4: (color online) Binder cumulant as a function of the inverse temperature for the isotropic disorder for several lattice sizes.

$U_4(\beta_{\text{cross}}(L, 2L), L) = U_4(\beta_{\text{cross}}(L, 2L), 2L)$ . In this paper (regarding the RAM) we will only show the results based on the analysis of the crossing temperatures of  $R_\xi$ , the so-called  $R_\xi$  channel. We have used a fifth-order polynomial-based analysis to compute the crossing temperatures.

Furthermore, we have computed the value of  $R_\xi$  at  $\beta_{\text{cross}}$ , the value of  $\nu_\xi$  from the behavior of  $\partial_\beta \xi$  (the behavior of  $\partial_\beta U_4$  will provide an additional estimate of the  $\nu$  exponent denoted as  $\nu_{U_4}$ ). Finally, we have also computed  $\eta$  from the behavior of the susceptibility ( $\chi$ ) and also the ratios  $Q_{U_4}$  and  $Q_{g_2}$ .

In the next two subsections we will discuss in detail our findings for the two disorder distributions.

TABLE I: Quotient method results for  $D = 3$  and  $D = 4$  and anisotropic disorder distribution (ARAM) from the crossing points of  $R_\xi$  at lattice sizes  $L_1$  and  $L_2$ .

$D$	$L_1/L_2$	$\beta_{\text{cross}}$	$R_\xi$	$\nu_\xi$	$\nu_{U_4}$	$\eta$	$Q_{U_4}$	$Q_{g_2}$
3	6/12	0.6992(2)	0.5485(6)	0.756(1)	0.747(2)	0.019(3)	0.9975(2)	1.31(4)
3	8/16	0.6993(2)	0.5486(9)	0.757(5)	0.77(1)	0.026(5)	0.9978(3)	1.44(5)
3	12/24	0.69940(8)	0.550(1)	0.740(4)	0.762(7)	0.031(5)	0.9975(3)	1.30(5)
3	16/32	0.69941(7)	0.549(1)	0.726(6)	0.75(1)	0.030(6)	0.9980(4)	1.00(5)
3	24/48	0.69932(7)	0.548(2)	0.737(8)	0.76(2)	0.03(1)	0.9983(6)	1.12(6)
4	6/12	0.7073(2)	0.5383(7)	0.740(2)	0.749(4)	0.027(4)	0.9954(2)	1.17(3)
4	8/16	0.7079(2)	0.540(1)	0.751(7)	0.78(1)	0.035(6)	0.9952(4)	1.38(5)
4	12/24	0.7083(1)	0.545(1)	0.734(5)	0.76(1)	0.033(7)	0.9962(5)	1.17(5)
4	16/32	0.7082(1)	0.542(2)	0.710(8)	0.71(2)	0.036(9)	0.9943(7)	1.20(6)
4	24/48	0.70830(7)	0.545(2)	0.733(9)	0.76(2)	0.04(1)	0.9947(9)	1.26(7)

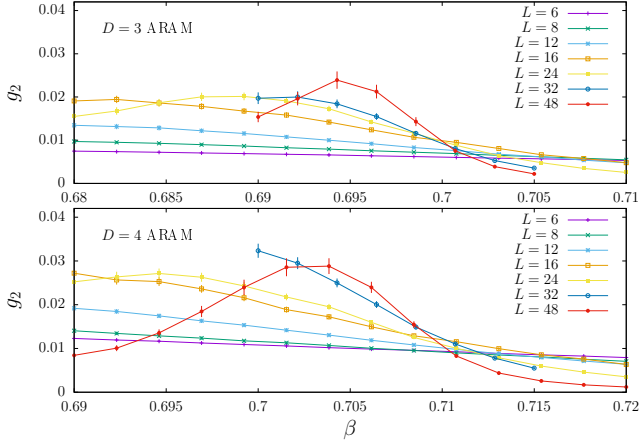


FIG. 5: (color online)  $g_2$  cumulant as a function of the inverse temperature for the cubic disorder for several lattice sizes.

#### A. Analysis of the cubic disorder results

We start describing our findings obtained using the quotient method.

The Binder cumulant analysis presents strong scaling corrections, therefore, we will present the results of the critical parameters obtained with the analysis of the crossing temperatures of  $R_\xi$ .

The data presented in Table I show almost negligible (in our numerical precision) corrections to scaling. Hence, we take the results for the largest pair (24 and 48) as our final estimate using the quotient method. We present the critical temperature,  $R_\xi$  cumulant at the critical point and correlation length and pair correlation function critical exponents,  $\nu$  and  $\eta$ , for  $D = 3$  and  $D = 4$  in Table II.

The non-monotonic behavior of the cumulants  $Q_{g_2}$  and  $Q_{U_4}$  (see Table I), for both values of  $D$ , precludes us to compute the  $\omega$  exponent.

We have also analyzed our numerical data using the fixed coupling method. We present our estimates in Ta-

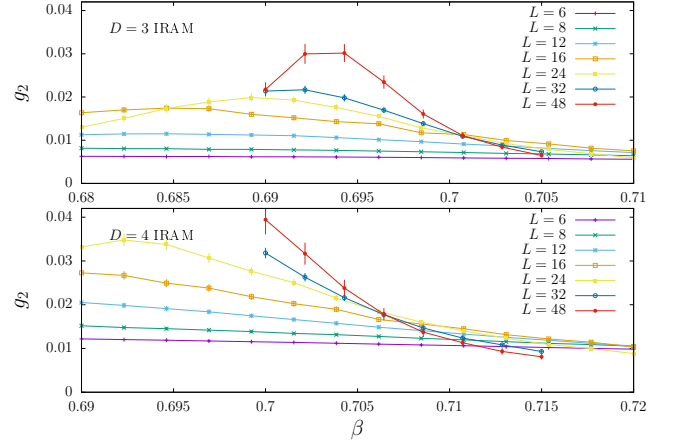


FIG. 6: (color online)  $g_2$  cumulant as a function of the inverse temperature for the isotropic disorder for several lattice sizes.

ble III. In this analysis we have only used the leading term: as in the quotient method we have been unable to characterize corrections to scaling (see Appendix B).

We would like to stress that the quotient and fixed coupling extrapolations are fully statistically compatible for each value of  $D$ . In addition, as a check of universality, it is important to state the statistical compatibility of all the four sets of extrapolated values (two different methods and two different values of  $D$ ).

Finally, the behavior of  $Q_{g_2}$  as a function of the lattice size (see Table I) is a strong hint for an asymptotic non zero value of  $g_2$  at the critical point, hence, ruling out that the ARAM belongs to the (pure) Heisenberg universality class for  $D = 3$  and 4.

#### B. Analysis of the isotropic disorder results

We have analyzed the isotropic disorder in the same way as the cubic one, focusing on the analysis of the crossing temperatures of  $R_\xi$  since the Binder data present

TABLE II: Critical temperature, exponents and  $R_\xi$  for the cubic disorder (ARAM),  $D = 3$  and 4, obtained with the quotient method analysis of the  $R_\xi$ -channel. As explained in the text, the Hamiltonian for  $D = 3$  and 4 shows small corrections to scaling, and we have quoted the results obtained from the biggest lattices (24 and 48).

$D$	$\beta_c$	$R_\xi$	$\nu_\xi$	$\nu_{U_4}$	$\eta$
3	0.69932(7)	0.548(2)	0.737(7)	0.76(2)	0.03(1)
4	0.70830(7)	0.545(2)	0.733(9)	0.76(2)	0.04(1)

TABLE III: Fixed coupling method results (as described in the Appendix B) for the cubic disorder (ARAM) and  $D = 3$  and 4. We have used  $R_\xi = 0.544$  for both values of  $D$ .

$D$	$R_\xi$	$\beta_c$	$\nu_\xi$	$\nu_{U_4}$	$\eta$
3	0.544	0.69941(5)	0.733(3)	0.76(5)	0.028(1)
4	0.544	0.70827(5)	0.736(3)	0.72(1)	0.035(3)

strong corrections to scaling.

In Tables V and VI we present the extrapolations of the isotropic disorder using i) the quotient method and ii) an analysis based in the behavior of the different data at a fixed coupling  $R_\xi$  near its asymptotic value. Notice that both analysis provide consistent results for the critical temperatures as well as for the critical exponents (considering the statistical errors). In addition, the study of the behavior of  $Q_{g_2}$  with the lattice size for both values of  $D$  provides us with the value  $\omega \simeq 1$ .

We have found that the  $\nu$  and  $\eta$  exponents are different for the two values of  $D$ . This fact may be due to a crossover effect or our statistical errors are masking scaling corrections. Moreover, the critical exponents and cumulants for  $D = 3$  and 4 are different from those of the cubic disorder. As for the cubic disorder, the behavior of  $Q_{U_4}$  and  $Q_{g_2}$  (see Table IV), for both values of  $D$ , provided strong support for an asymptotic non zero value for the cumulants, in particular that of  $g_2$ .

The non-zero value of  $g_2$  as well as the other values of the critical exponents and cumulants (Tables V and VI) significantly differ from those of the pure Heisenberg model (see Tables VII and X).

We finally remark that the  $\nu$  exponent is measurably growing with the disorder strength.

## V. CONCLUSIONS AND DISCUSSIONS

We have simulated the RAM with cubic and isotropic disorder in three dimensions. To do that, we have run very large numerical simulations using PT (and Metropolis as the local update method) simulating large lattice sizes ( $L = 48$ ).

This model was studied in Ref. [80] by means numerical simulations and using the PT algorithm for cubic and isotropic disorder distributions. The authors simulated only  $D = 4$  and  $L \leq 24$ . They found clear crossing of the different Binder cumulant curves for both distributions. Despite this, the authors claimed that the low temperature phase is in the QLRO class. They only computed the  $\nu$  exponent by studying the susceptibil-

ity, quoting for both disorders  $\nu = 0.70998$  with 0 as a statistical error, hence, claiming that both disorders belong to the same universality class. In addition they reported  $\beta_c = 0.70998(4)$  for ARAM and  $\beta_c = 0.70435(2)$  for IRAM. In this work, we report estimates of  $\beta_c$  and  $\nu$  for both disorders not compatible with those of Ref. [80].

In the previous section, we have discussed the critical behavior for both disorder distributions. Since it is clear that the critical behavior of these two distributions is different we will discuss separately our findings for each distribution.

### A. Cubic disorder

We have found a phase transition between a paramagnetic phase and a ferromagnetic one. Both values of the strength of the anisotropy,  $D$ , provide with critical exponents and cumulants compatible in the statistical error, fact which supports the universality of this disorder for moderate values of  $D$ .

Notice that our estimates for the critical exponents and cumulants are completely different from the Heisenberg model ones (see Table VII). Moreover, we have simulated the pure Heisenberg method using PT method, analyzing it using the same procedure applied to the ARAMs and IRAMs and it is clear they belong to different universality classes (see Table X of the Appendix C).

Furthermore our results do not agree with results of perturbative RG predictions [32, 33, 55–57, 59] which states that the ARAM should belong to the same universality class as the three-dimensional site-diluted Ising model (compare our values for the critical exponents from Tables II and III with the Monte Carlo results of Table VII for the three-dimensional site-diluted Ising model<sup>1</sup>).

<sup>1</sup> Data of Table VII for the site-diluted Ising model are corroborated also by RG studies, see e. g., Refs. [89–91].

TABLE IV: Quotient method results for  $D = 3$  and  $D = 4$  and isotropic disorder distribution (IRAM) from the crossing points of  $R_\xi$  at lattice sizes  $L_1$  and  $L_2$ .

$D$	$L_1/L_2$	$\beta_{\text{cross}}$	$R_\xi$	$\nu_\xi$	$\nu_{U_4}$	$\eta$	$Q_{U_4}$	$Q_{g_2}$
3	6/12	0.6975(2)	0.5540(8)	0.807(2)	0.768(2)	0.012(4)	0.9995(1)	1.64(4)
3	8/16	0.6977(2)	0.554(1)	0.828(6)	0.81(1)	0.015(5)	1.0008(2)	1.69(5)
3	12/24	0.6978(2)	0.556(2)	0.846(6)	0.83(1)	0.013(6)	1.0030(2)	1.40(5)
3	16/32	0.6980(2)	0.557(2)	0.87(1)	0.89(1)	0.00(1)	1.0049(4)	1.18(4)
3	24/48	0.6975(2)	0.552(3)	0.92(2)	0.90(2)	0.01(2)	1.0033(6)	1.4(1)
4	6/12	0.7060(3)	0.551(1)	0.896(4)	0.869(4)	-0.004(5)	1.0024(2)	1.36(2)
4	8/16	0.7065(3)	0.553(2)	0.98(1)	0.97(2)	-0.012(7)	1.0049(3)	1.31(4)
4	12/24	0.7055(3)	0.548(2)	0.98(1)	1.01(2)	-0.007(9)	1.0048(4)	1.28(4)
4	16/32	0.7052(2)	0.542(3)	0.97(2)	0.98(2)	-0.00(1)	1.0049(5)	1.14(4)
4	24/48	0.7055(3)	0.549(5)	1.13(5)	1.17(5)	-0.04(2)	1.0077(8)	1.04(7)

TABLE V: Independent extrapolations of the quotient method data (as describe in the text) for the isotropic disorder and for  $D = 3$  and 4. For the  $\nu$  exponents of the  $D = 4$  case we have been unable to extrapolate the data, since we quote the values of the largest pair.

$D$	$\beta_c$	$R_\xi$	$\nu_\xi$	$\nu_{U_4}$	$\eta$	$\omega$
3	0.6981(2)	0.556(2)	0.91(1)	0.94(2)	0.012(3)	$\sim 1$
4	0.7053(2)	0.543(9)	1.13(5)	1.17(5)	-0.013(16)	$\sim 1$

TABLE VI: Fixed coupling method results (as described in the Appendix B) for the isotropic disorder (IRAM) and  $D = 3$  and 4. We have used  $R_\xi = 0.55$  for  $D = 3$  and 0.54 for  $D = 4$ .

$D$	$R_\xi$	$\beta_c$	$\nu_\xi$	$\nu_{U_4}$	$\eta$
3	0.55	0.6977(1)	0.91(1)	0.94(2)	0.014(1)
4	0.54	0.7054(1)	1.010(5)	1.11(4)	-0.008(4)

TABLE VII: Critical exponents and cumulants for three three-dimensional related models.

Model	$\nu$	$\eta$	$\omega$	$R_\xi$	$U_4$	$g_2$
Heisenberg [92–94]	0.7116(10)	0.0378(3)	0.773	0.5639(2)	0.6202(1)	0
Ising (site-diluted) [95]	0.6837(53)	0.037(4)	0.37(6)	0.598(4)	0.449(6)	0.145(3)
Ising [96, 97]	0.629912(86)	0.0362978(20)	0.8303(18)	0.6431(1)	0.46548(5)	0

The following scenario emerges from our simulations: the anisotropic disorder, as predicted by RG, is relevant and changes the universality class of the pure model. We have checked that this scenario holds for  $D \leq 4$ . We expect this new fixed point should be relevant for  $0 < D < D_c$ . We can try to conjecture the behavior of the model with anisotropic disorder for strong anisotropy. For large  $D > D_c$  the anisotropic disorder will destroy the ferromagnetic phase and a spin glass phase will arise. We know that for  $D = \infty$  the system is described by the Ising spin glass universality class [70]. Open problems are the characterization of  $D_c$  and to figure out the universality class for  $D_c < D < \infty$ : is that of the Ising spin glass model in three-dimensions?

## B. Isotropic disorder

Regarding the isotropic disorder, the model again shows a clear (for the two values of  $D$  simulated) second order phase transition between a paramagnetic phase and a ferromagnetic one.

However, the two simulated values of  $D$  present very different critical exponents: this could be due to the corrections to scaling but both models could belong to different universality classes. Another possibility could be a crossover to a new universality class for larger lattice sizes. Or even that the scaling corrections have been masked by our statistical errors.

Notice that our estimates of the critical exponents and cumulants are different from the pure Heisenberg ones.

Our findings in this case are in striking conflict with different theoretical predictions which predict no phase

transition for this disorder distribution.

A recent analytical approach based on functional RG [50] has predicted a phase transition, like in the 2D XY-model, where this exponent is mathematically infinite, the low temperature phase showing QLRO.

In Appendix D we have studied the two dimensional  $O(2)$  model using the fixed coupling method as a proxy of models showing a QLRO phase. In agreement with the theory, the curves of the cumulants from our numerical simulations merge in a unique curve below the critical temperature, see Fig. 8, and consequently we have found very large  $\nu$  exponents, fact that we have not been able to see in the IRAMs ( $\nu \sim 0.9$  for  $D = 3$  and  $\nu \sim 1.1$  for  $D = 4$ )<sup>2</sup>. In addition, the curves of the different cumulants studied in this paper do not merge below the critical temperature. Hence, our numerical data do not support a QLRO low temperature phase for the largest simulated lattices.

The isotropic disorder description is much more involved since the state-of-the-art perturbative field theoretical RG [24] does not find a new fixed point describing the relevance of this disorder [31–33, 59]. However from our results we see that the disorder is relevant and that the systems present a phase transition from a paramagnetic phase to a ferromagnetic one. The limit for infinite strength of the disorder is again the three-dimensional Ising spin glass model [70].

The strong dependence of the  $\nu$  exponent on the disorder strength would mark the onset of the disappearance of the phase transition in the ferromagnetic channel. For example, the critical exponent in the Heisenberg model diverges as the system approaches from above its lower critical dimensions as  $\propto 1/(d-2)$ , being  $d$  the dimensionality of the system. The analogy in our model is  $D$  as a proxy for  $d$  in the pure model. If we assume that the  $\nu$  exponent is growing with  $D$  (this could change simulating larger lattices), one expects that the paramagnetic-ferromagnetic transition will disappear and a spin glass phase will appear for finite  $D$ .

How we can interpret the existence of a second-order phase transitions for the isotropic distribution?

Firstly, if Imry-Ma arguments are correct then we have studied small systems with sizes below the Imry-Ma-Larkin length. However, in that case we should expect effective critical behavior with exponents close to that of the Heisenberg universality class which is not the case. Such situation was observed in the numerical study of RAM with XY-spins, where critical exponents similar to those of the XY universality class were obtained except for the heat capacity critical exponent [74].

Secondly, the appearance of a Griffiths singularity in the system can invalidate the Imry-Ma analysis, as it was

interpreted in the case of random-field model [98].

A final possibility is the presence of a crossover (for  $L \gg 48$ ) to a QLRO phase despite the analysis presented in the Appendix D and our numerical results for the isotropic disorder.

## Acknowledgments

The authors acknowledge useful discussions with R. Folk, A. A. Fedorenko, L. A. Fernandez and V. Martin-Mayor. This work was partially supported by Ministerio de Economía y Competitividad (Spain) through Grants No. FIS2016-76359-P and PID2020-112936GB-I00, by Junta de Extremadura (Spain) through Grant No. GRU18079, IB16013 and IB20079 (partially funded by FEDER), Polish National Agency for Academic Exchange (NAWA) through the Grant No. PPN/ULM/2019/1/00160, National Academy of Sciences of Ukraine within the framework of the Project KIIKKB 6541030, and by European Union through Grant No. PIRSES-GA-2011-295302. We have run the simulations in the computing facilities of the Instituto de Biocomputación y Física de Sistemas Complejos (BIFI) and those of the Instituto de Computación Científica Avanzada (ICCAEx).

## Appendix A: Numerical Simulations details

We have performed extensive Monte Carlo numerical simulations using the Metropolis (with 10 hits) and PT algorithms, see Refs. [84, 85]. We have checked that the PT is correctly working with our choice of the different parameters.

In order to have an additional test of the thermalization of our systems, we have studied the behavior of different observables at all the temperatures as a function of  $\log t$  ( $t$  being the Monte Carlo time). We consider that we have thermalized the system, for a given observable, when the last three points are compatible in the error bars and a plateau can be defined (the last point is computed with the last half of the Monte Carlo history). All the results presented in this study fulfill this thermalization criteria.

In Tables VIII and IX we report the parameters used in the numerical simulations for the models with  $D = 3$  and 4 and both types of disorder, cubic and isotropic, namely, the number of disorder realizations  $N_{\text{samples}}$ , number of temperatures  $N_T$  and number of Monte Carlo sweeps  $N_{\text{sweeps}}$ .

## Appendix B: Quotient and fixed coupling methods

In this appendix we briefly describe the quotient and fixed coupling methods.

<sup>2</sup> In the  $D = 4$  case we have found  $\nu$  exponents a bit higher than expected, this fact has precluded us to extrapolate the  $\nu$  exponents to infinite volume (see Table V)

TABLE VIII: Parameters used in the numerical simulations for the cubic disorder distribution (ARAM).

$D$	$L$	$N_{\text{samples}}$	$N_{\text{T}}$	$N_{\text{sweeps}}$
3	6	13600	14	$10^5$
3	8	4800	14	$10^5$
3	12	2937	14	$10^5$
3	16	2000	14	$1.28 \times 10^5$
3	24	2091	14	$1.28 \times 10^5$
3	32	1400	8	$2.56 \times 10^5$
3	48	392	8	$5.12 \times 10^5$
4	6	13600	14	$10^5$
4	8	4800	14	$10^5$
4	12	2938	14	$10^5$
4	16	2000	14	$1.28 \times 10^5$
4	24	2068	14	$2.56 \times 10^5$
4	32	1400	8	$2.56 \times 10^5$
4	48	768	14	$5.12 \times 10^5$

TABLE IX: Parameters used in the numerical simulations for the isotropic disorder distribution (IRAM).

$D$	$L$	$N_{\text{samples}}$	$N_{\text{T}}$	$N_{\text{sweeps}}$
3	6	13600	14	$10^5$
3	8	4800	14	$10^5$
3	12	3000	14	$10^5$
3	16	2000	14	$1.28 \times 10^5$
3	24	2075	14	$1.28 \times 10^5$
3	32	1400	8	$2.56 \times 10^5$
3	48	400	8	$5.12 \times 10^5$
4	6	17600	14	$10^5$
4	8	4800	14	$10^5$
4	12	3000	14	$10^5$
4	16	2000	14	$1.28 \times 10^5$
4	24	2000	14	$2.56 \times 10^5$
4	32	1400	8	$2.56 \times 10^5$
4	48	400	8	$1.024 \times 10^6$

Firstly, we describe the quotient method. Let  $O(\beta, L)$  be a dimensionful quantity scaling in the thermodynamic limit as  $\xi^{x_O/\nu}$ . For a dimensionless observable the exponent  $x_O = 0$ . Thereafter, we will use the symbol  $g$  to denote all the dimensionless quantities, such as  $U_4$ ,  $g_2$  or  $R_\xi$ .

The behavior of the observable  $O$  can be studied by computing, at  $L$  and  $2L$ , the quotient

$$\mathcal{Q}_O = \frac{O(\beta_{\text{cross}}(L, 2L), 2L)}{O(\beta_{\text{cross}}(L, 2L), L)}, \quad (\text{B1})$$

where  $\beta_{\text{cross}}(L, 2L)$  is defined by

$$g(L, \beta_{\text{cross}}(L, 2L)) = g(2L, \beta_{\text{cross}}(L, 2L)). \quad (\text{B2})$$

From the previous discussion, one can write

$$\mathcal{Q}_O^{\text{cross}} = 2^{x_O/\nu} + \mathcal{O}(L^{-\omega}), \quad (\text{B3})$$

and

$$g^{\text{cross}} = g^* + \mathcal{O}(L^{-\omega}), \quad (\text{B4})$$

where  $x_O/\nu$ ,  $g^*$  and the correction-to-scaling exponent  $\omega$  being universal quantities. In order to compute the  $\nu$  and  $\eta$  exponents, one should study dimensionful observables such as the susceptibility ( $x_\chi = \nu(2 - \eta)$ ) and the  $\beta$ -derivatives of  $R_\xi$  and  $U_4$  ( $x = 1$  in both cases).

The crossing point of the inverse temperature ( $\beta_{\text{cross}}(L, 2L)$ ) behaves following the equation

$$\beta_{\text{cross}}(L, 2L) = \beta_c + A_{\beta_c, g} L^{-\omega-1/\nu} + \dots \quad (\text{B5})$$

The leading correction-to-scaling exponent can be computed via the quotient of a given dimensionless quantity  $g$  ( $Q_g$ ). The behavior of this quotient is

$$\mathcal{Q}_g^{\text{cross}}(L) = 1 + A_g L^{-\omega} + B_g L^{-2\omega} + \dots \quad (\text{B6})$$

Another way to compute critical exponents is to work at a fixed dimensionless observable. One fixes the value of the dimensionless observable  $g = g_f$  near the universal one (for example fixing a given value of  $R_\xi$ ) and then computes  $\beta(L)$  defined as

$$g_f = g(\beta(g_f, L), L). \quad (\text{B7})$$

Using these values of the inverse temperature, one can monitor the scaling. At this value of the inverse temperature we can study the scaling of different observables (e.g. susceptibility, derivatives of  $R_\xi$  and Binder cumulant, etc) to extract the critical exponents using

$$O(\beta(g_f, L), L) = A(g_f) L^{x_O/\nu} \left( 1 + \mathcal{O}\left(\frac{1}{L^\omega}\right) \right). \quad (\text{B8})$$

### Appendix C: The three-dimensional $O(3)$ model

In this appendix we present our results on the three-dimensional  $O(3)$  model using the quotient method with the same methodology as applied throughout the paper for the RAM.

We have run for this model  $L = 6, 12, 16, 24, 32$  and 48 lattices, using parallel tempering with eight temperatures in the fixed range  $[0.686, 0.700]$ .

In Tables X and XI we show the results of the quotient method for the crossing points of  $R_\xi$  and the Binder cumulant respectively (see also Fig. 7). First, we have computed  $\omega$  by fitting the last column to Eq. (B6). Once we have got this value, we perform all the fits of the rest of columns using this  $\omega$  value but for the inverse critical temperature (in this case, the correction is  $1/\nu + \omega$ , and we have left completely free this exponent in the fit). In

the last row of these tables we have reported our extrapolations to infinite volume. The agreement, despite the small lattice sizes simulated, with the values reported in Table VII, is pretty good. In addition, the inverse critical temperature is fully compatible with the one reported in Ref. [99] ( $\beta_c = 0.69300(1)$ ).

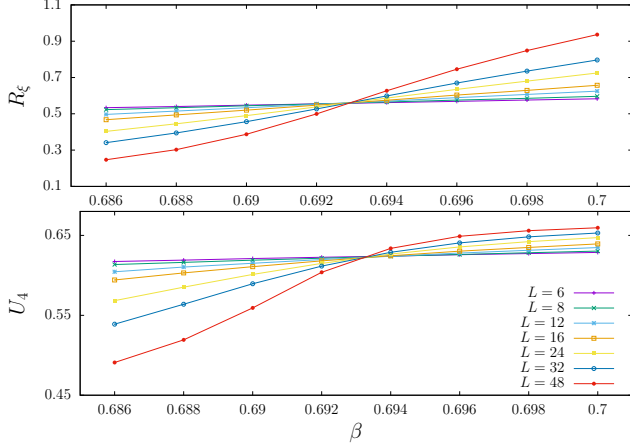


FIG. 7: (color online)  $R_\xi$  (top) and  $U_4$  (bottom) cumulants against inverse temperature for the three-dimensional  $O(3)$  pure model for several lattice sizes.

## Appendix D: The two-dimensional $O(2)$ model

In order to test the QLRO scenario for the IRAM, we have simulated the two-dimensional  $O(2)$  model.

The most accurate analysis of this model has been performed in Ref. [100] reporting  $\beta_c = 1.1199(1)$ ,  $R_\xi = 0.7506912$  and  $U_4 = 0.660603(12)$ .

We have analyzed this model by studying the  $R_\xi$  and  $U_4$  curves (see Fig. 8) using the fixed coupling method and neglecting scaling corrections. We report the results in Tables XII and XIII. One can see from Fig. 8 that the correlation length data suffer from larger corrections to scaling than the Binder cumulant ones. Notice that the  $U_4$  analysis provided with a value of the  $\eta$  exponent compatible with the analytical one ( $\eta = 1/4$ ). Moreover, the  $\nu$  exponents take very large values, eventually diverging in the thermodynamic limit, showing the fact that different curves of  $R_\xi$  and  $U_4$  are merging in the low temperature phase, which presents QLRO behavior.

- [1] See *e.g.* Q. Duo, D.Q. Ahoy, M.X.Pan, W. H. Wang, Appl. Phys. Lett. **92**, 011923 (2008); Q. Luo, W. H. Wang, J. Non-Crystalline Solids, **355**, 759 (2009); Q. Luo, B.Schwartz, N. Mattern, J. Eckert, J. Appl. Phys. **109**, 113904 (2011).
- [2] J. Hertz, Phys. Scr **T10**, 1 (1985).
- [3] Yu. Holovatch, V. Blavats'ka, M. Dudka, C. von Ferber, R. Folk, T. Yavors'kii, Int. J. Mod. Phys. B. **16**, 4027 (2002).
- [4] R. Harris, M. Plischke, M. J. Zuckermann, Phys. Rev. Lett. **31**, 160 (1973).
- [5] R. W. Cochrane, R. Harris, M. J. Zuckermann, Phys. Reports **48**, 1 (1978).
- [6] D.J. Sellmyer, M. J. O'Shea, in: D. H. Ryan (Ed.), *Recent progress in random magnets*, p. 71 (World Scientific, Singapore, 1992).
- [7] Y. Goldschmidt, in: D. H. Ryan (Ed.), *Recent progress in random magnets*, p. 151 (World Scientific, Singapore, 1992).
- [8] M. Dudka, Yu. Holovatch, R. Folk, J. Magn. Mater. **294**, 305 (2005)
- [9] J.M.D. Coey, J. Appl. Phys. **49**, 1646 (1978).
- [10] For review see E. M. Chudnovsky, in: J. A. Fernandez-Baca, W.-Y. Ching (Eds.), *The Magnetism of Amorphous Metals and Alloys*, p. 143 (World Scientific, Singapore, 1992).
- [11] V. L. Berezinski, Sov. Phys. JETP **32** 493 (1971); V. L. Berezinski, Sov. Phys. JETP **34**, 610 (1972).
- [12] J. M. Kosterlitz, D. J. Thouless, J. of Phys. C **6**, 1181 (1983).
- [13] U. Krey, Z.Physik B **26**, 355 (1977); U. Krey, J. Magn.

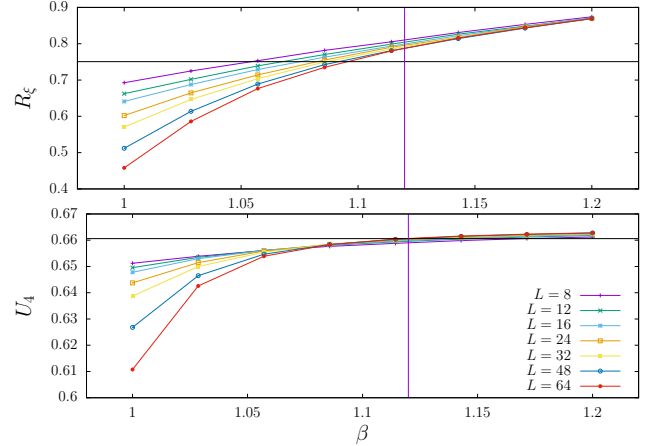


FIG. 8: (color online)  $R_\xi$  and  $U_4$  cumulants versus inverse temperature for the two dimensional  $O(2)$  pure model on different lattice sizes. We have also plotted  $\beta_c = 1.1199(1)$ ,  $R_\xi = 0.7506912$  and  $U_4 = 0.660603(12)$ .

Magn. Mater. **7**, 150 (1978); C. De Dominicis, Phys. Rev. B **18**, 4913 (1978); S.-k. Ma, J. Rudnick, Phys. Rev. Lett. **40**, 589 (1978); A. Khurana, Phys. Rev. B **25**, 452 (1982); S. Ciuchi, F. de Pasquale, Nucl. Phys. B **300** [FS22], 31 (1988); D.R.C. Dominguez, W. K. Theumann, J. Phys. A **28**, 63 (1995); M. Dudka, R. Folk, Yu. Holovatch, G. Moser, Condens. Matter Phys.

TABLE X: Quotient method results for the pure  $O(3)$  model ( $D = 0$ ) from the crossing points of  $R_\xi$  at lattice sizes  $L_1$  and  $L_2$ . The numbers in round brackets are the statistical error of the fit and the number inside the square ones are systematic errors originating from the uncertainty in the  $\omega$  exponent used in the fit.

$L_1/L_2$	$\beta_{\text{cross}}$	$R_\xi$	$\nu_\xi$	$\nu_{U_4}$	$\eta$	$Q_{U_4}$
6/12	0.692577(7)	0.5567(5)	0.727(3)	0.697(7)	0.024(2)	0.9966(3)
8/16	0.69283(3)	0.5587(3)	0.718(3)	0.699(5)	0.029(2)	0.9972(2)
12/24	0.69290(2)	0.5597(5)	0.716(3)	0.705(7)	0.034(2)	0.9982(2)
16/32	0.69293(2)	0.5601(4)	0.714(4)	0.706(7)	0.037(2)	0.9986(2)
24/48	0.69298(1)	0.5617(4)	0.717(6)	0.72(1)	0.036(3)	0.9990(3)
$\infty$	0.6930(3)	0.5630(5)[6]	0.708(4)[2]	0.717(9)[2]	0.043(2)[2]	$\omega = 0.92(13)$

TABLE XI: Quotient method results for pure  $O(3)$  model from the crossing points of  $U_4$  at lattice sizes  $L_1$  and  $L_2$ . The numbers between round brackets are the statistical error of the fit and the number inside the square ones are systematic errors originating from the uncertainty in the  $\omega$  exponent used in the fit.

$L_1/L_2$	$\beta_{\text{cross}}$	$U_4$	$\nu_\xi$	$\nu_{U_4}$	$\eta$	$Q_{U_4}$
6/12	0.6942(1)	0.6243(2)	0.731(8)	0.728(3)	-0.015(3)	1.0168(7)
8/16	0.69368(5)	0.6236(1)	0.720(6)	0.718(2)	-0.003(2)	1.0130(6)
12/24	0.69320(3)	0.6223(2)	0.721(8)	0.716(3)	0.017(2)	1.0083(8)
16/32	0.69309(2)	0.6217(1)	0.720(8)	0.714(4)	0.021(2)	1.0064(8)
24/48	0.69305(2)	0.6214(1)	0.72(1)	0.716(6)	0.025(3)	1.005(1)
$\infty$	0.69300(3)	0.6202(2)[2]	0.707(3)[1]	0.72(1)[1]	0.042(3)[3]	$\omega = 0.98(9)$

TABLE XII: Independent extrapolations of the fixed coupling method data, using the Binder cumulant  $U_4 = 0.6606$ , for the two dimensional XY model.

$U_4$	$\nu_\xi$	$\nu_{U_4}$	$\eta$
0.6606	3.8(2)	3.6(3)	0.246(3)

TABLE XIII: Independent extrapolations of the fixed coupling method data, using  $R_\xi = 0.75$ , for the two dimensional XY model.

$R_\xi$	$\nu_\xi$	$\nu_{U_4}$	$\eta$
0.75	4.0(1)	7.0(6)	0.236(1)

- 8, 737 (2005); M. Dudka, R. Folk, Yu. Holovatch, G. Moser, J. Phys. A **40**, 8247 (2007).
- [14] A. Fedorenko, F. Kühnel, Phys. Rev. B **75**, 174206 (2007).
- [15] A. Fedorenko, Phys. Rev. E **86**, 021131 (2012).
- [16] E. Callen, Y. J. Liu, J. R. Cullen, Phys. Rev. B **16**, 263 (1979); J. D. Patterson, G. R. Gruzalski, D. J. Sellmyer, Phys. Rev. B **18**, 1377 (1978).
- [17] R. Harris, D. Zobin, J. Phys. F **7**, 337 (1977).
- [18] B. Derrida and J. Vannimenus, J. Phys. C **13**, 3261 (1980).
- [19] N. Sourlas, J. de Phys. Lett. (France) **42**, 233 (1981).
- [20] M.A. Continentino, Coutinho, J. Magn. Magn. Mater. **125**, 49 (1993).
- [21] K.H. Fischer, Phys. Rev. B **36**, 6963 (1987).
- [22] Y. Imry, S.-k. Ma, Phys. Rev. Lett. **35**, 1399 (1975).
- [23] R. Alben, J. J. Becker, and M. C. Chi, J. Appl. Phys. **49**, 1653 (1978).
- [24] D. J. Amit and V. Martín Mayor, *Field Theory, The Renormalization Group and Critical Phenomena*, (World Scientific Publishing, 2005).
- [25] A. Aharony, Phys. Rev. B **12**, 1038 (1975).
- [26] J.-H. Chen, T. C. Lubensky, Phys. Rev. B **16**, 2106 (1977).
- [27] R.A. Pelcovits, E. Pytte, J. Rudnick, Phys. Rev. Lett. **40**, 476 (1978).
- [28] R. A. Pelcovits, E. Pytte, J. Rudnick, Phys. Rev. Lett. **48**, 1297, (1982).
- [29] R. A. Pelcovits, Phys. Rev. B **19**, 465 (1979).
- [30] V. J. Emery, Phys. Rev. B **11**, 239 (1975).
- [31] M. Dudka, R. Folk, Yu. Holovatch, Condens. Matter Phys. **4**, 77 (2001).
- [32] M. Dudka, Yu. Holovatch, R. Folk, in: W. Janke, A. Pelster, H.-J. Schmidt and M. Bachmann (Eds.), *Fluctuating Paths and Fields*, Singapore, World Scientific, 2001, p. 457.
- [33] P. Calabrese, A. Pelissetto, E. Vicari, Phys. Rev. E **70**, 036104 (2004).
- [34] E. F. Shender, J. Phys. C **13**, L339 (1980).
- [35] R. Fisch, A. B. Harris, J. Appl. Phys. **67**, 5778 (1990).
- [36] R. Fisch, A. B. Harris, Phys. Rev. B **41**, 11305 (1990).
- [36] A. B. Harris, R. G. Caflisch, J. R. Banavar, Phys. Rev.

- B **35**, 4929 (1987).
- [37] Y. Y. Goldschmidt, Nucl. Phys. B **225** [F59], 123 (1983).
  - [38] A. Khurana, A. Jagannathan, M. J. Kosterlitz, Nucl. Phys. B **240** [F312], 1 (1984).
  - [39] Y. Y. Goldschmidt, Phys. Rev. B **30**, 1632 (1984).
  - [40] A. Jagannathan, B. Schaub, M. J. Kosterlitz, Nucl. Phys. B **265** [F515], 324 (1986).
  - [41] D. Boyanovsky, Nucl. Phys. B **225** [FS9], 523 (1983).
  - [42] D. S. Fisher, Physica A **177**, 84 (1991).
  - [43] A. M. Khorunzhy, B. A. Khorunzhenko, L. A. Pastur, M. V. Shcherbina, in: C. Domb, J. L. Lebowitz (Eds.), *Phase Transitions and Critical Phenomena*, Vol. **15**, p.74 (Academic Press, London, 1992).
  - [44] A. Aharony, E. Pytte, Phys. Rev. Lett **45**, 1583 (1980).
  - [45] A. Aharony, E. Pytte, Phys. Rev. B **27**, 5872 (1983).
  - [46] J. Villian, J. F. Fernandez, Z. Phys. B **54**, 139 (1984).
  - [47] V. S. Dotsenko, M. V. Fieglman, J. Phys. C **16**, L803 (1983).
  - [48] D. E. Feldman, JETP Lett. **70**, 135 (1999); D. E. Feldman, Phys. Rev. B **61**, 382 (2000); D. E. Feldman, Int. J. Mod. Phys. B **15**, 2945 (2001).
  - [49] D. S. Fisher, Phys. Rev. B **31**, 7233 (1985).
  - [50] M. Tissier, G. Tarjus, Phys. Rev. B **74**, 214419 (2006).
  - [51] P. Le Doussal, K. J. Wiese, Phys. Rev. Lett. **96**, 197202 (2006).
  - [52] Y. Sakamoto, H. Mukaida, C. Itoi, Phys. Rev. B **72**, 144405 (2005); Y. Sakamoto, H. Mukaida, C. Itoi, Phys. Rev. B **74**, 064402 (2006); Y. Sakamoto, H. Mukaida, C. Itoi, J. Phys.: Condens. Matter **19**, 145219 (2007);
  - [53] K. Ideura, Prog. of Theor. Phys. **119**, 9 (2008); K. Ideura, Prog. of Theor. Phys. **121**, 897 (2009).
  - [54] D. Mouhanna, G. Tarjus, Phys. Rev. B **94**, 214205 (2016).
  - [55] M. Dudka, R. Folk, Yu. Holovatch, Condens. Matter Phys. **4**, 459 (2001).
  - [56] D. Mukamel, G. Grinstein, Phys. Rev. B **25**, 381 (1982).
  - [57] A. L. Korzhenevskii and A. A. Luzhkov, Zh. Eksp. Teor. Fiz. **94**, 250 (1988)[Sov. Phys. JETP **67**, 1229 (1988)].
  - [58] V. Dubs, V. Prudnikov, and P. Prudnikov, Theoret. and Math. Phys. **190**, 359 (2017).
  - [59] D. Shapoval, M. Dudka, A. A. Fedorenko, Yu. Holovatch, Phys. Rev. B **101**, 064402 (2020).
  - [60] K. H. Fischer, A. Zippelius, J. Phys. C **18**, L1139 (1985).
  - [61] K. H. Fischer, A. Zippelius, Prog. Theor. Phys. **87**, 165 (1986).
  - [62] D.R.C. Dominguez and W. K. Theumann, Phys. Rev. B **48**, 6234 (1993).
  - [63] M. C. Chi, R. Alben, J. Appl. Phys. **48** (1977) 2987.
  - [64] R. Harris, S. H. Sung, J. Phys. F **8**, L299 (1978).
  - [65] M. C. Chi, T. Egami, J. Appl. Phys. **50**, 1651 (1979).
  - [66] R. Harris, J. Phys. F **10**, 2545 (1980) .
  - [67] C. Jayaprakash, S. Kirkpatrick, Phys. Rev B **21**, 4072 (1980).
  - [68] A. Chakrabarti, Phys. Rev. B **36**, 5747 (1987).
  - [69] R. Fisch, Phys. Rev. B **39**, 873 (1989).
  - [70] F. Parisien Toldin, A. Pelissetto, E. Vicari, J. Stat. Mech. P06002 (2006).
  - [71] R. Fisch, Phys. Rev. Lett. **66**, 2041 (1991).
  - [72] R. Fisch, Phys. Rev. B **42**, 540 (1990) .
  - [73] P. Reed, J. Phys. C **24**, L117 (1991).
  - [74] U. K. Rößler, Phys. Rev. B **59**, 13577 (1999) .
  - [75] M. Itakura, Phys. Rev. B **68**, 100405(R) (2003).
  - [76] R. Fisch, Phys. Rev. B **79**, 21449 (2009).
  - [77] R. Fisch, Phys. Rev. B **48**, 15764 (1993) .
  - [78] R. Fisch, Phys. Rev. B **58**, 5684 (1998).
  - [79] R. Fisch, Phys. Rev. B **51**, 11507 (1995).
  - [80] H. M. Nguyen, P.-Y. Hsiao, J. Appl. Phys. **105**, 07E125 (2009)
  - [81] A. I. Larkin, Zh. Eksp. Teor. Fiz. **58**, 1466 (1970) [Sov. Phys. JETP **31**, 784 (1970)].
  - [82] A.A. Berzin, A.I. Morosov, A.S. Sigov, Phys. Solid State **58**, 2018 (2016).
  - [83] A.A. Berzin, A.I. Morosov, A.S. Sigov, Phys. Solid State **59**, 2448 (2017); A.A. Berzin, A.I. Morosov, A.S. Sigov, J. Magn. Magn. Mater. **459**, 256 (2018).
  - [84] K. Hukushima and K. Nemoto, J. Phys. Soc. Japan **65**, 1604 (1996).
  - [85] E. Marinari in *Advances in Computer Simulation* edited by J. Kerstész and I. Kondor (Springer Verlag, 1998).
  - [86] F. Cooper, B. Freedman and D. Preston, Nucl. Phys. B **210**, 210 (1982).
  - [87] H.G. Ballesteros, L.A. Fernandez, V. Martin-Mayor, A. Munoz-Sudupe, G. Parisi and J. J. Ruiz-Lorenzo. Nuclear Physics B **512**, 681 (1998).
  - [88] S. Wiseman and E. Domany, Phys. Rev. E **52**, 3469 (1995); A. Aharony and A. B. Harris, Phys. Rev. Lett. **77**, 3700 (1996).
  - [89] A. Pelissetto, E. Vicari, Phys.Rept **368**, 549 (2002)
  - [90] R. Folk, Y. Holovatch, T. Yavors'kii, Physics Uspekhi **173**, 175 (2003)
  - [91] M. V. Kompaniets, A. Kudlis, and A. I. Sokolov, Phys. Rev. E **103**, 022134 (2021)
  - [92] M. Campostrini, A. Pelissetto, P. Rossi and E. Vicari Phys. Rev. E **65**, 066127 (2002).
  - [93] M. Hasenbusch and E. Vicari, Phys. Rev. B **84**, 125136 (2011).
  - [94] M. Hasenbusch, J. Phys. A: Math. Gen. **34**, 8221 (2001)
  - [95] H.G. Ballesteros, L.A. Fernandez, V. Martin-Mayor, A. Munoz-Sudupe, G. Parisi and J. J. Ruiz-Lorenzo, Phys. Rev. B. **58**, 2740 (1998).
  - [96] A. M. Ferrenberg, J. Xu and D. P. Landau, Phys. Rev. E **97**, 043301 (2018),
  - [97] D. Simmons-Duffin, J. High Energ. Phys. **86**, 88 (2017).
  - [98] R. Fisch, Phys. Rev. B **76**, 214435 (2007).
  - [99] H. G. Ballesteros, L. A. Fernandez, V. Martin-Mayor and A. M. Sudupe, Phys. Lett. B **387**, 125 (1996).
  - [100] M. Hasenbusch, J. Phys. A **38**, 5869 (2005); M. Hasenbusch, J. Stat. Mech: Theor. and Exp. P08003 (2008).